RSC Advances

ROYAL SOCIETY OF CHEMISTRY

www.rsc.org/advances

Journal Name

RSCPublishing

ARTICLE

Multifunctional iron oxide/silk-fibroin (Fe_3O_4-SF) composite microspheres for the delivery of cancer therapeutics

Cite this: DOI: 10.1039/x0xx00000x

Received 00th January 2012,
Accepted 00th January 2012

DOI: 10.1039/x0xx00000x

www.rsc.org/

Haiyun Zhang, Xilan Ma*, Chuanbao Cao*, Meina Wang, Youqi Zhu

In this article, we report novel multifunctional iron oxide/silk-fibroin (Fe_3O_4-SF) microspheres synthesized by simple salting out process. These microspheres are subsequently loading doxorubicin hydrochloride (a traditional anti-cancer drug), denoted as DOX-Fe_3O_4-SF. The results show that the drug loading capacity (LC) is 3.3% and the drug encapsulation efficiency (EE) could reach to 76%. The DOX-loaded microspheres exhibit sustained and pH-sensitive release patterns. The total DOX release is measured to be about 60% at pH = 5.5. More interestingly, RhB-labelled Fe_3O_4-SF microspheres exhibit a striking endocytosis, selectively accumulating in the cytoplasm compared to the free RhB. The endocytosis of DOX-Fe_3O_4-SF microspheres results in only ~10% survival ratio of Hela cells after 48 h. Furthermore, due to remarkable biocompatibility of SF, Fe_3O_4-SF microspheres show none cytotoxicity toward Hela cells compared to DOX-Fe_3O_4-SF. The results clearly indicate that Fe_3O_4-SF microspheres hold great potential for drug loading and delivery into cancer cells to induce cell death.

1. Introduction

Since last few centuries, cancer remains to be a major health problem worldwide. Statistical results have confirmed that ~25% mortality rate[1] is due to the cancer in United States. Outside the awful truth, fortunately, cancer-therapy drugs have been proposed to be efficient treatment strategy through a controllable release manner[2-4]. However, cancer-therapy drugs often accompany with toxic side effects and suffer from a low targeted drug delivery efficiency limitation. It is still a great challenge to transport the anti-cancer drugs exactly to the targeted place for avoiding the damage of healthy tissues[5-7]. This issue has attracted great interest in synthesis of appropriate drug delivery system with high tumour targeting efficiency.

Nanostructured magnetic Fe_3O_4（Fe_3O_4 NPs）, widely used in various biomedical fields due to biocompatibility, can provide potential platform for targeted drug delivery. Forced by external (or internally implanted) magnetic fields, the magnetic nanoparticles can be manipulated to selectively targeting the affected organs or tissues[8-14]. However, despite the advantages, it is important to understand the toxicity of Fe_3O_4 NPs. Some reports have found that excess accumulation of iron ions would damage neuronal in the brain or could affect protein synthesis in neural cells[15-17]. For improving the cytocompatibility of Fe_3O_4 NPs, combining with carriers to form multifunctional composites is required. Multifunctional composites are potential platforms for many applications, such as for cancer therapy. Moreover, such a composite could be used for treating hyperthermia, bioimaging[18]. Many ligands have been developed to improve multifunctional drug delivery, for example, silica, organic polymers[19-20]. Yanna Cui et al. have demonstrated that the magnetic PLGA NPs loaded with DOX are effective for brain glioma treatment. Jinjin Shi et al. have reported PEGylated fullerene multi-functional magnetic nanocomposites are possible cure for cancer theranostic[21-22]. These results indicate that this kind of multifunctional composites is very promising for targeted drug delivery. However, most targeting ligands are synthetic polymers and it is difficult to modify them. On the other hand, natural polymers have attracted attention primarily because they are similar to biological macromolecules, often biocompatible or even biodegradable, and relatively inexpensive, which permits the potential for chemical or physical modification[23-24].

As a natural, fibrous protein produced by a variety of insects and spiders, silk fibroin is further used for drug delivery with sustainable release properties. In particular, silk fibroin holds quite similarity biological macromolecules, remarkable biocompatibility and controllable degradability, demonstrating

a preferred biomedical material[25-26]. Above all, silk presents negative charge because it comprises of 39% glycine and 34% alanine[27] in solution with pH > 4. In addition, the cytocompatibility of Fe_3O_4 NPs will increase due to fact that the surface charge of magnetic NPs will decrease by combination with SF[28]. So this is of great significance to prepare multifunctional iron oxide/silk-fibroin composites for drug delivery. Actually, the preparation of magnetic silk composites have been reported in 1998[29] and it is of great significance to scientific research. However, their main focus has been on the modification of spider silk fibers. Recently, Fe_3O_4 NPs coated with SF has been reported, but the report mostly focused on the modification of Fe_3O_4 NPs by SF solution. There is a limited number of reports exploring conjugation of SF and Fe_3O_4 NPs to obtain multifunctional composites for the potential of targeted drug delivery. On the other hand, designing a composite with selectivity to cells, although challenging, is of great importance for research and therapy of many serious diseases[30-31]. Fe_3O_4-PEG–FITC–CNT composites have been reported to locate at the perinuclear region of MCF7 cells[18, 32], but the synthetic methods of the composites are complex. Efforts have been made to investigate endocytosis of silk composites, but few reports were about multifunctional iron oxide/silk-fibroin composites. For example, Shuying Yu[33] et al. have prepared FUDR-loaded SF nanospheres, but endocytosis experiment shows the nanocarriers only adhere onto the Hela cells. Although Joydip Kundu[34] have reported silk nanoparticles prepared by desolvation could be endocytosed by cells. However, targeted agents (such as Fe_3O_4 NPs) were not found in silk nanoparticles and they might not actively target the cancerous cells. Therefore, simple synthesis of multifunctional iron oxide/silk-fibroin composites and the composites could be endocytosed by Hela cells are required for the potential of targeted drug delivery.

Herein, novel multifunctional iron oxide/silk-fibroin composites are fabricated via simple salting out process. Doxorubicin hydrochloride (DOX) is loaded into the Fe_3O_4-SF microspheres and the drug release properties are examined. More importantly, we were surprised to find that the multifunctional iron oxide/silk-fibroin composites exhibited a striking endocytosis and could selectively accumulate in the cytoplasm of Hela cells. The effects of these composite microspheres on cell cytotoxicity are also evaluated by using Hela cells.

2 Experimental

2.1 Silk fibroin solutions

Bombyx mori fibroin solution was prepared following previously published procedures[35-38]. Silk was boiled for 30 minutes in 0.02 M Na_2CO_3 solution and the same procedure was repeated twice to degum the glue-like sericin coating. The extracted silks fibroin were dissolved in $CaCl_2/H_2O/CH_3CH_2OH$ solution (mole ratio, 1:8:2) at 80℃. Then the fibroin solution was dialyzed with dialysis cassettes (molecular weight cut-off, 14,000) against distilled water for 3 days to yield fibroin aqueous solution.

2.2 Synthesis of Fe_3O_4 nanoparticles

In the experimental, $Fe_2(SO_4)_3$ (17.5 ml, 0.25 mol/L) and $FeSO_4$ (10 ml, 0.5 mol/L) were mixed in a single-neck flask. $NH_3 \cdot H_2O$ was added into the solution and pH of the solution was adjusted to ~10[39]. The mixture was magnetically stirred for 30 minutes and kept at room temperature for a week. Then the resultant black solution was matured for 30 minutes at 80℃. The precipitation was washed thoroughly with distilled water and ethanol. Nanoparticles were obtained after drying at 60℃ in vacuum oven.

2.3 Synthesis of Fe_3O_4-SF, DOX-Fe_3O_4-SF and RhB-labelled Fe_3O_4-SF microspheres

Fe_3O_4-SF microspheres were prepared by mixed solution salting out from potassium phosphate (pH=9)[40]. 0.5wt% SF solution and 0.5wt% Fe_3O_4 solution were mixed in a volume ratio of 40:1. Then the mixed solution was added into 1.25M potassium phosphate solution in volume ratio of 1:5. The mixture was incubated at 4℃ for 2 h and kept at room temperature for 12 h. The precipitation was collected and washed thoroughly with distilled water. Fe_3O_4-SF microspheres were obtained by freeze-drying.

Preparation process of DOX-Fe_3O_4-SF microspheres was simple. Fe_3O_4-SF microspheres (80mg/10ml) dispersed into PBS were mixed with different concentrations of DOX solution (0.15, 0.25, 0.35 and 0.5 mg/ml). The mixed system was stirred at room temperature for 12 h, the precipitation was collected and washed thoroughly with PBS to remove residual DOX. Composites were obtained by freeze-drying. The collected supernatant was analyzed by UV-Vis spectrometry to calculate the drug loading capacity (LC) and drug encapsulation efficiency (EE). LC and EE was calculated as follows:

$$LC(\%) = \frac{The\ amount\ of\ drugs\ by\ adsorption}{The\ amount\ of\ carriers} \times 100$$

$$EE(\%) = \frac{initial\ amount\ of\ drugs - drugs\ in\ supernatant}{initial\ amount\ of\ drugs} \times 100$$

RhB-labelled composite microspheres are prepared by adsorption. Fe_3O_4-SF microspheres (80mg/10ml) dispersed into PBS were mixed with RhB solution (0.15mg/ml). The mixed system was stirred at room temperature for 12 h, the precipitation was collected and washed thoroughly with PBS to remove residual RhB. Composites were obtained by freeze-drying.

2.4 Characterization

The shapes and crystalline structures of Fe_3O_4 NPs were characterized by Transmission electron microscopy (TEM) and

high resolution transmission electron microscopy (HRTEM). The magnetic property of samples was investigated by vibrating sample magnetometer (VSM). The morphology of the composite microspheres was analyzed by scanning electron microscopy (SEM). X-ray diffraction (XRD) curves were recorded to analyze crystalline structure of samples.

2.5 In vitro drug release

DOX-Fe_3O_4-SF microspheres (50 mg) and PBS (10 ml, pH=5.5, 7.4) were added into dialysis cassettes. Dialysis cassettes were sealed at both ends and immersed into 90 ml PBS (pH=5.5, 7.4, 37℃). At set time increments, 10 ml of the supernatant was collected and replaced with an equal volume of fresh PBS solution. The collected supernatant was analyzed by UV-Vis spectrometry.

2.6 Cellular uptake investigation

Laser confocal investigation was applied to examine the localization of composite microspheres into cells. The free RhB and RhB-labelled Fe_3O_4-SF microspheres were added into Hela cells respectively and they were co-cultured for 4 h. Then the cells were washed three times with PBS to eliminate residues. The cells were fixed with 4% paraformaldehyde for 15 minutes. Finally, cells were analyzed for red fluorescence by confocal microscope analysis.

2.7 MTS assay

The cell metabolic activity was measured by MTS. Hela cells were maintained in DMEM medium supplemented with 10% fetal bovine serum. The cells were cultured at 37℃ in a humidified atmosphere of 5% CO_2. Hela cells in accordance with the density of 5,000 cells per well were seeded in 96-well plates. Medium (100μl) prepared with different concentrations of the sample solution (200, 100, 50, 25, 12.5, 6.25 and 3.125 μg/ml) was added to each well. The cells with medium were cultured for 24 h and 48 h at 37℃. 20 μl MTS was added to each well and the system was kept 4 h, then each well was determined for absorbance at 490 nm.

3 Results and discussion

3.1 Fe_3O_4 NPs structural analysis

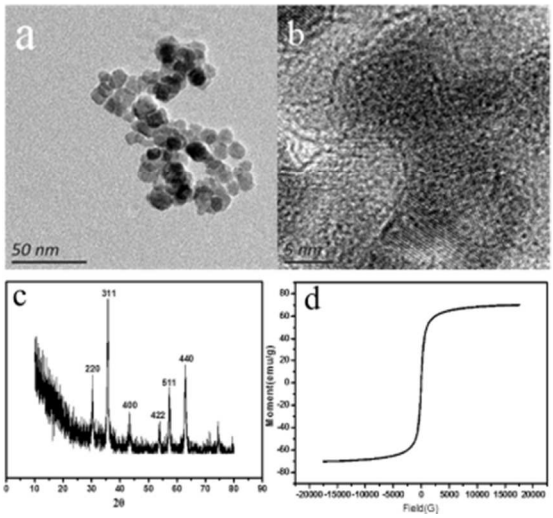

Fig.1 TEM images of as-prepared Fe_3O_4 NPs (a), HRTEM images (b), XRD of as-prepared Fe_3O_4 NPs (c) and Hysteresis loops of the as-prepared Fe_3O_4 NPs (d).

Fig.1a showed TEM images of as-prepared Fe_3O_4 NPs. The size distribution of Fe_3O_4 NPs is uniform and the mean diameter size is 15 ± 2 nm (Fig.1a). To test the crystalline properties of magnetic nanoparticles, high resolution transmission electron microscopy(HRTEM) analysis was examined. In HRTEM images of Fig.1b, the lattice fringes were clearly found and the result showed Fe_3O_4 NPs hold great crystalline properties. The phase identification of Fe_3O_4 NPs was characterized by XRD. There existed strong diffraction peaks corresponding to the crystal planes of (220), (311), (400), (422), (511) and (440) of crystalline Fe_3O_4 NPs, respectively (Fig.1c). The results showed that Fe_3O_4 NPs held the trans-spinel phase structure. Magnetization measurements recorded with VSM were performed in order to examine the magnetic behavior of Fe_3O_4-NPs. In Fig.1d, the specific saturation magnetization value of Fe_3O_4 NPs was measured to be 70.15 emu/g and there was almost no magnetic hysteresis. The results demonstrate that Fe_3O_4 NPs are superparamagnetic as previously reported[41-42].

3.2 Morphology and properties of Fe_3O_4-SF microspheres

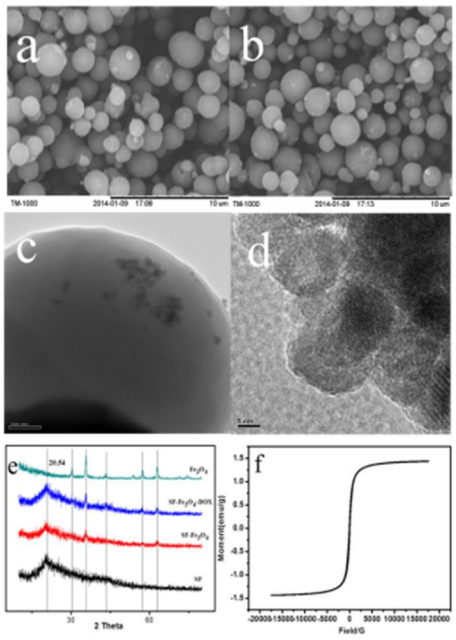

Fig.2 The morphology of Fe_3O_4-SF (a) and after loading DOX (b), TEM images (c) and HRTEM images (d) of as-prepared Fe_3O_4-SF, XRD of as-prepared composite microspheres (e) and Hysteresis loops of DOX-Fe_3O_4-SF composite microspheres (f).

Fig.2a depicts SEM picture of the composite microspheres. The aqueous-derived microspheres showed a relatively rough surface and size ranged from 500±50 to 3000±200 nm. Some small bumps were found on the surface and this might be caused by iron oxide aggregation. To verify this hypothesis, the composites were measured by TEM and HRTEM. From Fig.2c, inhomogenous distribution of Fe_3O_4 NPs in composites could be clearly found. This phenomenon result from the magnetic attraction force of Fe_3O_4 NPs. But clear lattice fringes and uniform size distribution of Fe_3O_4 NPs demonstrated magnetic nanoparticles were not affected by silks (Fig.2d). Fig.2b showed the surface of composites had no obvious change after loading DOX. This might because a small amount of DOX was absorbed into microspheres. To investigate changes in structure of silks, XRD analysis was measured. In Fig.2e, all microspheres exhibited a mostly β-sheet structure ($2\theta=20.5^\circ$) and similar crystalline properties. The results indicated that silk II crystalline structure existed in the composites and Fe_3O_4 NPs had no effect on silk structure. Magnetic behavior of the composites was examined by VSM. The saturated magnetization was about 1.5 emu/g and there was almost no magnetic hysteresis in Fig.2f. The saturated magnetization of composites was smaller than pure Fe_3O_4 NPs because a small amount of magnetic nanoparticles was added into silk solution. The quality percentage of Fe_3O_4 NPs was analyzed by TGA (Figure S1). Therefore, we have successfully synthesized magnetic iron oxide/silk-fibroin composite microspheres and the composites provide possibility for targeted drug delivery.

3.3 Loading efficiency

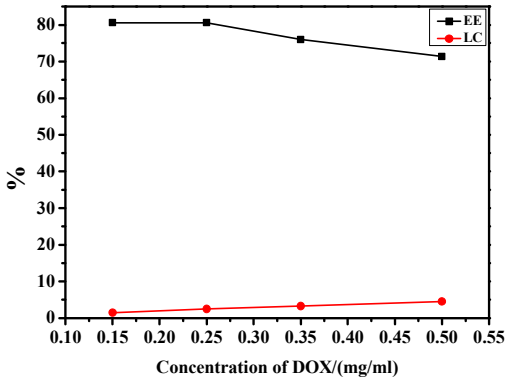

Fig.3 The drug loading capacity (LC) and drug encapsulation efficiency (EE) under different DOX concentrations.

The drug loading capacity (LC) and drug encapsulation efficiency (EE) are important to evaluate the availability of the carriers. As shown in Fig.3, different concentrations of DOX solution were used to obtain the appropriate LC and EE. The LC increased with the increase of DOX concentration, but the EE decreased under the same conditions. According to the trends of curves, the LC could reach to the biggest point under one DOX concentration. Whereas the EE changed smaller than the former that it could not conform to the requirements of the cost. Therefore, the suitable DOX concentration was 0.35 mg/ml, the LC and EE respectively were 3.3%, 76%.

3.4 In vitro drug release

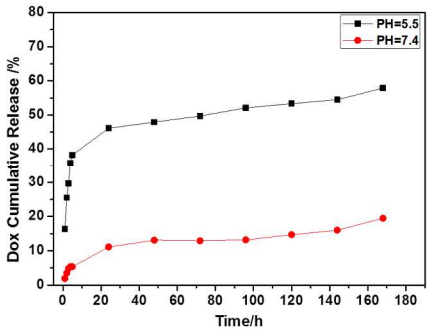

Fig.4 DOX released from DOX-Fe_3O_4-SF composite microspheres under different pH conditions.

pH is an important factor[43], as it exists naturally in cells of pathological change, as well as cancer cells. Therefore, DOX release at different pH was investigated. As shown in Fig.4, DOX-Fe_3O_4-SF microspheres exhibited sensitive response to pH. The in vitro release showed that about 60% of DOX was released at pH 5.5, whereas DOX release was less than 20% at pH 7.4 under the same conditions. This might result from the presence of strong hydrogen bonding force interactions between composites and DOX at pH 7.4. Under acid conditions[44], H^+ in solution could compete with the hydrogen bond forming group and weaken hydrogen bond interactions. Furthermore, both DOX and silk carry positive charge in H^+ solution, which provides the necessary repulsion between them.

So DOX was released more at pH 5.5 than 7.4. Otherwise, DOX released from the composites kept sustained release for long time. These results demonstrate the Fe_3O_4-SF composite microspheres could be used for drug delivery.

3.5 Confocal assay

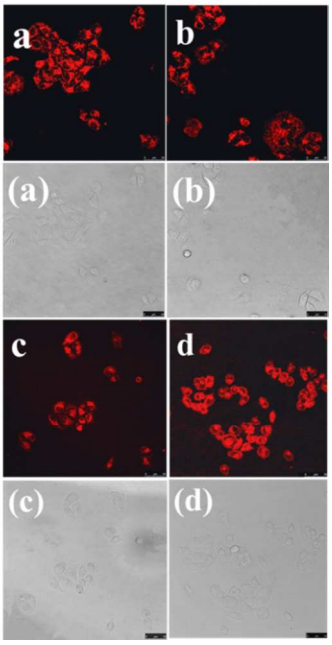

Fig.5 Confocal microscopic images of Hela cells with free RhB (a) (b) and RhB-labelled composite microspheres (c) (d) (12.5 μg/ml) in different regions.

The uptake of the RhB-labelled composite microspheres by Hela cells was observed using fluorescence and confocal microscopy. Fig.5 (c) (d) showed that the cellular cytoplasm was stained with red fluorescence soon after 4 h of incubation revealing cellular internalization of the RhB-labelled composite microspheres. It was clearly visible that the red fluorescence in cellular cytoplasm was focused on together, which result from the magnetic attraction of Fe_3O_4-SF composites. In contrast, cells treated with free RhB showed discursive red fluorescence internalized in the cellular cytomembrane and cytoplasm. These results indicated the RhB-labelled composite microspheres could be uptaken by Hela cells. Interestingly, the cells remained viable after incubation with for 4 h. The results testify composite microspheres hold no cytotoxicity effect on Hela cells. Compared with previous studies, this is a progress that we have successfully synthesized multifunctional iron oxide/silk-fibroin composites under few reports and the composites could be uptaken by Hela cells, which provides potential for the targeted drug delivery.

3.6 MTS assay

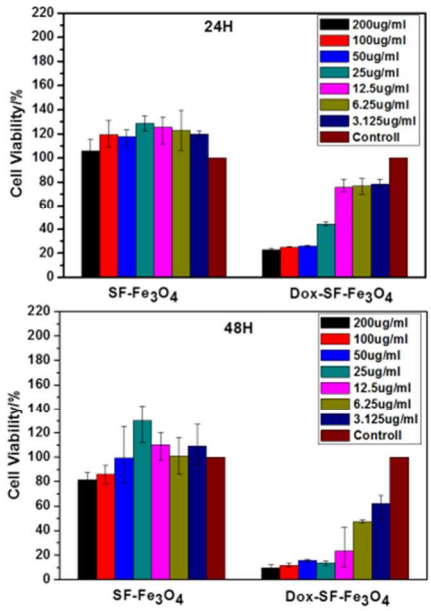

Fig.6 Effect of composite microspheres on the viability of HeLa cells, as measured by MTS.

To testify whether the released DOX was pharmacologically active, the cytotoxic effect of the DOX-Fe_3O_4-SF composite microspheres on HeLa cells was investigated. Fig.6 showed the viability of Hela cells incubated with Fe_3O_4-SF and DOX-Fe_3O_4-SF composite microspheres for 24 h and 48 h. The results showed the cytotoxicity of DOX-Fe_3O_4-SF increased with the increase of concentrations and DOX-Fe_3O_4-SF held greater cytotoxicity than Fe_3O_4-SF. On the other hand, only ~10% Hela cells were survival after co-culture with DOX-Fe_3O_4-SF for 48 h. This might be attributed to the release of DOX inside cells. Otherwise, the cytotoxicity of DOX-Fe_3O_4-SF increased with the increase of exposure on cells. This might because more DOX was released inside cells with the time increasing. Interestingly, the Fe_3O_4-SF exhibited no indication of cytotoxicity on Hela cells due to remarkable biocompatibility of silk fibroin. The results showed multifunctional Fe_3O_4-SF composite microspheres hold great potential for targeted drug delivery.

4. Conclusions

In summary, we suggest novel multifunctional iron oxide/silk-fibroin composite microspheres prepared via a simple salting out process. DOX was successfully loaded into Fe_3O_4-SF composite microspheres, which presented sustained and pH-sensitive release patterns. The total DOX release is measured to be about 60% at pH=5.5. More interestingly, the multifunctional iron oxide/silk-fibroin composites exhibited a striking endocytosis and could selectively accumulate in the cytoplasm of Hela cells, which provided possibility for research and therapy of many serious diseases. MTS results reveal that Fe_3O_4-SF microspheres with different concentrations had no

cytotoxicity due to remarkable biocompatibility of silk fibroin. However, DOX-Fe_3O_4-SF microspheres exhibit greater cytotoxicity toward Hela cells and only ~10% Hela cells are survival after 48 h incubation due to the release of DOX inside cells. The results clearly indicate that the Fe_3O_4-SF microspheres hold great potential in application of targeted drug delivery.

Research Centre of Materials Science, School of Materials Science and Engineering, Beijing Institute of Technology, Beijing 100081, P. R. China.
†*Corresponding Author Email: maxilan@bit.edu.cn, cbcao@bit.edu.cn (Chuanbao Cao)
Tel: +86 10 68913792 Fax: +86 10 68912001

References

[1] R. Siegel, D. Naishadham and A. Jemal, CA CANCER J CLIN, 2013, **63**, 11.
[2] Y. Chen, H. R. Chen, S. J. Zhang, F. Chen, L. X. Zhang, J. M. Zhang, M. Zhu, H. X. Wu, L. M. Guo, J. W. Feng and J. L. Shi, Adv. Funct. Mater. , 2011, **21**, 270.
[3] Vlerken LE and Amiji MM., Expert Opin Drug Deliv., 2006, **3**, 205.
[4] P. Huang, Z. M. Li, J. Lin, D. P. Yang, G. Gao, C. Xu, L. Bao, C. L. Zhang, K. Wang, H. Song, H. Y. Hu and D. X. Cui, Biomaterials, 2011, **32**, 3447.
[5] L. L. Li, Y. Q. Guan, H. Y. Liu, N. J. Hao, T. L. Liu, X. W. Meng, C. H. Fu, Y. Z. Li, Q. L. Qu, Y. G. Zhang, S. Y. Ji, L. Chen, D. Chen and F. Q. Tang, ACS NANO., 2011, **5**, 7462.
[6] B. Subia, S. Chandra, S. Talukdar and S. C. Kundu, Integr. Biol., 2014, **6**, 203.
[7] S. D. Steichen, M. C. Moore and N. A. Peppas, European Journal of Pharmaceutical Sciences, 2013, **48**, 416.
[8] F. Danhier, O. Feron and V. Préat, J.Control. Release, 2010, **148**, 135.
[9] T. Lammers, W. E. Kiessling and G. Storm, Mol.Pharmacol., 2010, **7**, 1899.
[10] C. H. Wang, S. T. Kang and C. K. Yeh, Biomaterials, 2013, **34**, 1852.
[11] L. P. Mazor, G. R. Dakwar, M. Popov, S. Kolusheva, A. Shames, C. Linder, S. Greenberg, E. Heldman, D. Stepensky and R. Jelinek, International Journal of Pharmaceutics, 2013, **450**, 241.
[12]J. M. Hu, Y. F. Qian, X. F. Wang, T. Liu and S. Y. Liu, Langmuir, 2012, **28**, 2073.
[13] K.J. Thompson, S. Shoham and J.R. Connor, Brain Res. Bull., 2011, **55**, 155.
[14] J. D. Blackwell, V. I. Shubayev, R. R. Fiñones and S.G. Jin, Biomaterials, 2007, **28**, 2572.
[15] K.J. Thompson, S. Shoham and J.R. Connor, Brain Res. Bull, 2001, **55**, 155.
[16] L. Zecca, M.B.H. Youdim, P. Riederer, J.R. Connor and R.R. Crichton, Nat. Rev. Neurosci, 2004, **5**, 863.
[17] T.R.I.I. Pisanic, J.D. Blackwell, V.I. Shubayev, R.R. Finones and S. Jin, Biomaterials, 2007, **28**, 2572.
[18] J. J. Khandare, A. J. Badhwar, S. D. Satavalekar, S. G. Bhansali, N. D. Aher, F. Kharas and S. S. Banerjee, Nanoscale, 2012, **4**, 837.
[19] J. Lu, M. L. Jeffrey. Zink. and F. Tamanoi, Small, 2007, **3**, 1341.
[20] H. Freichels, F. Danhier, V. Préat, P. Lecomte and C. Jérôme, Int. J. Artif. Organs, 2011, **34**, 152.
[21] J. J. Shi, X. Y. Yu, L. Wang, Y. Liu, J. Gao, J. Zhang, R. Ma, R. Y. Liu and Z. Z. Zhang, Biomaterials, 2013, **34**, 9666.
[22] N. Schleich, P. Sibret, P. Danhier, B. Ucakar, S. Laurent, R.N. Muller, C. Jérôme, B. Gallez, V. Préat and F. Danhier , International Journal of Pharmaceutics, 2013, **447**, 94.
[23] P. B. Malafaya, G. A. Silva, R. L. Reis, P.B. Malafaya, G.A. Silva and R.L. Reis, Adv. Drug Del. Rev., 2007, **59**, 207.
[24] J. A. Kluge, O. Rabotyagova, G. G. Leisk and D. L. Kaplan, Trends Biotechnol., 2008, **26**, 244.
[25] C. Veparia and D. L. Kaplan, Prog. Polym. Sci., 2007, **32**, 991.
[26] Q. Lv, C. B. Cao, Y. Zhang, X. L. Ma and H. S. Zhu, Journal of Materials Science: Materials in Medicine， 2004, **15**, 1193.
[27] G. X. Zhang and C. Li, Acta Sericol. Sinica., 2009, **35**, 99.
[28] D. H. Yan, G. F. Yin, Z. B. Huang, M. Yang, X. M. Liao, Y. Q. Kang, Y. D.Yao, B. Q. Hao and D. Han, J. Phys. Chem. B., 2009, **113**, 6047.
[29] E. L. Mayes, F.Vollrath and S. Mann, Adv. Mater., 1998, **10**, 801.
[30] B. Kang, M. A. Mackey and M. A. El-Sayed, J. Am. Chem. Soc., 2010, **132**, 1517.
[31] L. Rajendran, H. J. Knolker and K. Simons, Nat. Rev. Drug Discovery, 2010, **9**, 29.
[32] D. Depan and R. D. K. Misra, Nanoscale, 2012, **4**, 6325.
[33] S. Y. Yu, W. H.Yang, S. Chen, M. J. Chen, Y. Z. Liu, Z. Z.Shao and X. Chen, RSC Adv., 2014**,** **4**, 18171.
[34] J. Kundu, Y. Il Chung, Y. H. Kim, G. Tae and S.C. Kundu, International Journal of Pharmaceutics, 2010, **388**, 242.
[35] J. Zhou, C. B. Cao and X. L. Ma, International Journal of Biological Macromolecules, 2009, **45**, 504.
[36] X. H. Zhang, C. B. Cao, X. L. Ma and Y. N. Li, J Mater Sci: Mater Med., 2012, **23**, 315.
[37] Q. Lu, S. J. Zhang, K. Hua, Q. L. Feng, C. B. Cao and F. Z. Cui, Biomaterials, 2007, **28**, 2306.
[38] J. Zhou, C. B. Cao, X. L. Ma and J. Lin, International Journal of Biological Macromolecules, 2010, **47**,514.
[39] S. Laurent, D. Forge, M. Port, A. Roch, C. Robic, L. V. Elst and R. N. Muller, Chem. Rev., 2008, **108**, 2064.
[40] A. S. Lammel, X. Hu, S. H. Park, D. L. Kaplan and T. R. Scheibel, Biomaterials, 2010, **31**, 4583.
[41] M. V. Kovalenko, M. I. Bodnarchuk, R. T. Lechner, G. Hesser, F. Schäffler and W. Heiss, J. Am. Chem. Soc., 2007, **129**, 6352.
[42] F. X. Redl, C. T. Black, G. C. Papaefthymiou, R. L. Sandstrom, M. Yin, H. Zeng, C. B. Murray and S. P. O'Brien, J. Am. Chem. Soc., 2004, **126**, 14583.
[43] R. Cheng, F. H. Meng, C. Deng, H. A. Klok and Z. Y. Zhong. Biomaterials, 2013, **34**, 3647.
[44] B. Subia, S. Chandra, S. Talukdar and S. C. Kundu, Integr. Biol., 2014, **6**, 203.

